

- de-Loisy, E.; Damiens, A. The Manufacture of Alcohol or Ether from Ethylene Obtained from Coal Gas. *Chim. Ind.* 1923 (special no. May), 664-670; *Chem. Abstr.* 1923, 17, 3318.
- Doraiswamy, L. K.; Sharma, M. M. *Heterogeneous Reactions*. Wiley: New York, 1984; Vol. II.
- Engelhardt, R.; Lommel, W.; Ossenbeek, A. Treating Ethylene with Sulfuric Acid. U.S. Patent 1458646, 1923; *Chem. Abstr.* 1923, 17, 2587.
- Harris, H. G.; Himmelblau, D. M. Determination of Ethyl Hydrogen Sulfate, Diethyl Sulfate and Sulfuric Acid in Diethyl Sulfate Solutions. *Anal. Chem.* 1961, 33, 1764-1767.
- Harris, H. G.; Himmelblau, D. M. Kinetics of the Reactions of Ethylene with Sulfuric Acid—Reaction of Ethylene with Sulfuric Acid and Ethyl Hydrogen Sulfate. *J. Phys. Chem.* 1963, 67, 802-805.
- Harris, H. G.; Himmelblau, D. M. Kinetics of the Reaction of Ethylene with Sulfuric Acid. *J. Chem. Eng. Data* 1964, 9, 61-65.
- Hellin, M.; Jungers, J. C. *Bull. Soc. Chim. Fr.* 1957, 386-400.
- Jhaveri, A. S.; Sharma, M. M. Kinetics of Absorption of Oxygen in Aqueous Solutions of Cuprous Chloride. *Chem. Eng. Sci.* 1967, 22, 1-6.
- Joachim, B. E.; Paul, H.; Erich, K.; Wolfgang, S. Use of 1-Ethoxy-4-Ethylbenzene as a Scent and a Flavouring. Ger. Offen. DE 3128987, 1983; *Chem. Abstr.* 1983, 98, 124531.
- Maimeri, C. The Preparation of Ethyl Alcohol and Diethyl Sulfate from Ethylene. *Chem. Abstr.* 1925, 19, 1402.
- Miller, S. A. *Ethylene and its Industrial Derivatives*. Ernest Benn Ltd.: London, 1969; Part II.
- Oyeveaar, M. H.; Westerterp, K. R. Mass Transfer Phenomena and Hydrodynamics in Agitated Gas-Liquid Reactors and Bubble Columns at Elevated Pressure: State of the Art. *Chem. Eng. Process.* 1989, 25, 85-98.
- Oyeveaar, M. H.; Delarie, T.; Sluijs, C.; Westerterp, K. R. Interfacial Areas and Gas Hold-ups in Bubble Columns and Packed Bubble Columns at Elevated Pressures. *Chem. Eng. Process.* 1989, 26, 1-14.
- Plant, S. G. D.; Sidgwick, N. V. The Absorption of Ethylene and Propylene by Sulfuric Acid. *J. Soc. Chem. Ind.* 1921, 40, 14T-18T.
- Schmidt, R. J. Hydration of Olefins. U.S. Patent 4393256, 1983; *Chem. Abstr.* 1983, 99, 157822.
- Truchard, A. M.; Harris, H. G. Solubility and Thermodynamic Functions of Ethylene in Diethyl Sulfate. *J. Phys. Chem.* 1961, 65, 575-576.

Received for review April 10, 1990

Revised manuscript received August 15, 1990

Accepted September 4, 1990

## Kinetic Studies on the Catalytic Decomposition of Hydrogen Sulfide in a Tubular Reactor

Vassilios E. Kaloidas and Nickos G. Papayannakos\*

Laboratory of Chemical Process Engineering, Department of Chemical Engineering, National Technical University of Athens, Iroon Polytechniou 9, GR-157 73 Zografou, Athens, Greece

The kinetics of hydrogen sulfide decomposition on catalyst  $\text{MoS}_2$  is studied with the use of a tubular reactor. Data were obtained in the temperature range 1013-1133 K, pressure range 1.3-3.1 atm, and feed specific flow rate range  $2.8 \times 10^{-4}$ - $3.5 \times 10^{-3}$  mol/(s·cm<sup>2</sup>). A Hougen-Watson adsorption model is adopted to represent the reaction mechanism. Analysis of the data indicates that the rate-determining step of the decomposition reaction is the cleavage of hydrogen-sulfur bonds of the hydrogen sulfide adsorbed on the catalyst active sites. The kinetic parameters and their dependence on temperature are determined. The dependence of the catalyst irreversible deactivation on the reaction temperature is presented and discussed.

### Introduction

The catalytic decomposition of hydrogen sulfide toward hydrogen and sulfur production has become a subject of considerable investigation in the past fifteen years due to the effective utilization of  $\text{H}_2\text{S}$ . This strong pollutant is either produced as an unavoidable by-product in processes of heavy oil hydrodesulfurization and coal gasification or obtained from sour natural gases. Research and development of hydrogen energy technology is also interested in the decomposition reaction of hydrogen sulfide. The advantage of the decomposition process compared to the conventional Claus process is the production of hydrogen besides sulfur. Hydrogen is a valuable product used as raw material in the chemical industry and as a clean fuel to produce energy at high temperatures.

In an early work, Kingman (1936) carried out  $\text{H}_2\text{S}$  decomposition experiments over a heated molybdenum filament in the temperature range from 673 to 1138 K. A first-order reaction kinetics with respect to  $\text{H}_2\text{S}$  partial pressure and an activation energy of 25 kcal/mol are mentioned.

Searching for an effective catalyst for the  $\text{H}_2\text{S}$  decomposition reaction, Kotera et al. (1974, 1977) and Fukuda et al. (1978) have compared the catalytic activities of the

compounds  $\text{FeS}$ ,  $\text{CoS}$ ,  $\text{NiS}$ ,  $\text{MoS}_2$ , and  $\text{WS}_2$  at temperatures and pressures ranging from 773 to 1073 K and from 0.08 to 0.13 atm respectively.  $\text{FeS}$ ,  $\text{CoS}$ , and  $\text{NiS}$  were sulfurized to  $\text{FeS}_2$ ,  $\text{CoS}_2$ , and  $\text{NiS}_2$  and presented negligible catalytic activity. An activation energy of 26.8 kcal/mol was calculated from the initial rates of  $\text{H}_2\text{S}$  decomposition using  $\text{MoS}_2$  powder (specific area 4.1 m<sup>2</sup>/g) as a catalyst. A greater catalytic activity of  $\text{MoS}_2$  is reported compared to that of  $\text{WS}_2$ . Using two different  $\text{MoS}_2$  charges, the first one at temperature 823 K for 180 h and the second one at 1073 K for 15.5 h, no significant changes of the catalytic activity at each temperature have been observed.

Raymont (1974, 1975) carried out experiments using a commercial Co/Mo catalyst in a quartz reactor cell and reports a  $\text{H}_2\text{S}$  catalytic decomposition activation energy of 8 kcal/mol.

Chivers et al. (1980) compared the catalytic activities of some metal sulfide powders in a quartz reaction cell at temperatures ranging between 673 and 1073 K. They propose as active catalysts for  $\text{H}_2\text{S}$  decomposition the compounds  $\text{Cr}_2\text{S}_3$  (specific area 13.4 m<sup>2</sup>/g),  $\text{MoS}_2$  (3.7 m<sup>2</sup>/g), and  $\text{WS}_2$  (5.5 m<sup>2</sup>/g).

In the up-to-date kinetic studies of the  $\text{H}_2\text{S}$  catalytic decomposition no reaction mechanism has been suggested and the reverse reaction has not been taken into account.

Various substances (such as Pt, Pd,  $\text{Al}_2\text{O}_3$ , red P) are referred to (Pascal, 1960) as catalysts of the  $\text{H}_2\text{S}$  synthesis

\* Author to whom correspondence should be addressed.

**Table I. Characteristics of the Two MoS<sub>2</sub> Catalyst Beds**

	bed 1	bed 2
dry catalyst mass, g	0.1026	0.1786
bed length, ( $L_{\text{cat}}$ ), cm	0.27	0.47
bed diameter ( $d_b$ ), cm		0.60
bed apparent density ( $d_b$ ), g/cm <sup>3</sup>		1.36
bed void fraction ( $\epsilon_b$ )		0.45
particle diameter range, cm	0.0315–0.0400	0.0250–0.0315
particle apparent density, g/cm <sup>3</sup>		2.46
particle pore volume, cm <sup>3</sup> /g		0.19
particle peak pore diameter (unimodal pore size distribution), Å		1950
particle specific area, m <sup>2</sup> /g		4.96

from hydrogen and sulfur. Zazhigalov et al. (1975) report the following activity order determined from experiments carried out in the temperature range of 453–693 K: CoS<sub>2</sub> > NiS = WS<sub>2</sub> > MoS<sub>2</sub> > FeS<sub>2</sub> > Ag<sub>2</sub>S > CuS > CdS > MnS > ZnS. They have also suggested a first-order reaction kinetics with respect to hydrogen concentration when these sulfides are used as catalysts.

The scope of the present work is to study the kinetics of H<sub>2</sub>S catalytic decomposition using MoS<sub>2</sub> as a catalyst and taking into account the reverse reaction and to propose a decomposition mechanism in the temperature range from 1013 to 1133 K and pressure range from 1.3 to 3.1 atm.

### Experimental Section

The experimental setup used for the kinetic study of catalytic decomposition of hydrogen sulfide and the determination of the temperature profiles inside the reactor are described elsewhere (Kaloidas and Papayannakos, 1989). A gas-tight alumina tube of 0.6-cm inner diameter and of 40.3-cm length was used as a catalytic reactor and was operated in a continuous mode. The feed of the reactor was 99.6% mol/mol H<sub>2</sub>S supplied by LINDE. Propane 0.08% mol/mol, propene 0.30% mol/mol, and a nitrogen–oxygen mixture 0.02% mol/mol were also contained as impurities in the feed. A modified Orsat analyzer (Kaloidas, 1988) was used for the determination of hydrogen content in the reactor effluent gas after the sulfur had been condensed and removed from the stream. To ensure that the main impurities propane and propene did not influence the kinetic studies, the existence of their possible product CS<sub>2</sub> in the effluent gas was investigated. The absence of CS<sub>2</sub> from the reactor exit gas was assured by a UV–vis photometric method (Kaloidas, 1988). The measurements of the hydrogen content was not influenced by the presence of the impurities propane and propene as they are both water soluble and thus easily removed from the measured volume of hydrogen. The accuracy of the mole/mole hydrogen content measurements, which coincide with the mole/mole hydrogen sulfide conversions, lies in the range of  $\pm 2\%$  of the measured value, in all the measurements made in this study.

Molybdenum disulfide was provided by VENTRON GmbH in a powder form. Two catalyst beds were built in the region of the maximum temperature inside the reactor tube (Kaloidas and Papayannakos, 1989) with characteristics given in Table I. The catalyst particle preparation was carried out by pressing at 292 atm and subsequent grinding of the formed slabs and screening of the particles. The two fractions collected from screening 0.0315–0.0400 cm and 0.0250–0.0315 cm with sieves of the series DIN 4188 were dried at 633 K, weighed, and used for the preparation of the two catalyst beds. These beds were supported at both ends by sintered alumina particles

of the same size as the catalyst ones. The supports ensured that the flow was well developed before it reached the catalyst section and excluded possible maldistributions at the catalyst bed exit. From mercury porosimetry measurements it was found that both fractions appeared to have the same pore structure and surface area. Nitrogen adsorption porosimetry experiments did not indicate the existence of micropores with diameters less than 150 Å.

Calculated values of catalytic particle effectiveness factor, assuming particle tortuosity  $\delta_{\text{cat}} \leq 2.8$  and taking into account that  $D_{\text{e,H}_2\text{S}} = 0.3 \text{ cm}^2/\text{s}$  (Kaloidas, 1988), were greater than 0.93.

Calculated values of Reynolds numbers for the bed particles were  $Re_p \geq 4$ , indicating  $Pe_L \approx 2$  and  $Pe_r \approx 10$  (Carberry, 1976; Rase, 1977). These values assure the legitimacy of the plug flow idealization for the catalyst beds. The test of the criterion for less than 5% influence of axial dispersion on the estimated reaction rate values

$$\frac{L_{\text{cat}}}{d_p} > \frac{1}{0.05} \frac{n_o}{Pe_L} \ln \frac{C_{\text{in}}}{C_{\text{out}}}$$

also suggested the acceptance of the plug flow model (Froment and Bischoff, 1979; Rase, 1977). The absence of axial dispersion and interparticle diffusional effects was also experimentally verified by the use of two catalyst beds, the longer one built with the smaller in size particles (Table I). The indicated reaction rates by either of the beds for certain reaction conditions did not differ within the range of the experimental conditions. Wall flow tendency can be considered insignificant because  $d_r/d_p \geq 15$  (Rase, 1977).

For all the empty sections of the tube the application of the noncatalytic model is used (Kaloidas and Papayannakos, 1989).

### Results and Discussion

**Catalyst Activity.** It was found that catalyst activity changed during experimentation. The below described method used for the determination of the remaining catalyst activity was independent on the hydrogen sulfide decomposition kinetic models.

In the region of small conversions when the reactor works in a differential mode, the decomposition rates along the catalyst bed can be considered constant. Thus, the dependence of the reaction rates on the conversions for tubular reactors can be described by the linear function

$$r_{\text{w,H}_2\text{S}} = \frac{F_{0,\text{H}_2\text{S}}}{V_{\text{cat}}} x(t, T, P_t, F_{0,\text{H}_2\text{S}}) \quad (1)$$

For the remaining catalyst activity,  $\alpha_{\text{cat}}$ , after a reaction time  $t$ , holds:

$$\alpha_{\text{cat}} = \frac{r_{\text{w,H}_2\text{S}}(t, T, P_t, F_{0,\text{H}_2\text{S}})}{r_{\text{w,H}_2\text{S}}(t=0, T, P_t, F_{0,\text{H}_2\text{S}})} = (\alpha_{\text{cat}})_f b_{\text{cat}} \quad (2)$$

where

$$(\alpha_{\text{cat}})_f = \frac{x(t \geq t_m, T, P_t, F_{0,\text{H}_2\text{S}})}{x(t=0, T, P_t, F_{0,\text{H}_2\text{S}})} \quad (3)$$

$t_m$  is time after which the catalyst activity remains constant.

$$b_{\text{cat}} = \frac{x(t, T, P_t, F_{0,\text{H}_2\text{S}})}{x(t \geq t_m, T, P_t, F_{0,\text{H}_2\text{S}})} \quad (4)$$

During experimentation, the conversion of hydrogen sulfide was determined with gradual increase of the reaction temperature from 1013 to 1133 K, as shown in Figures 1 and 2. Three levels of catalyst remaining activity

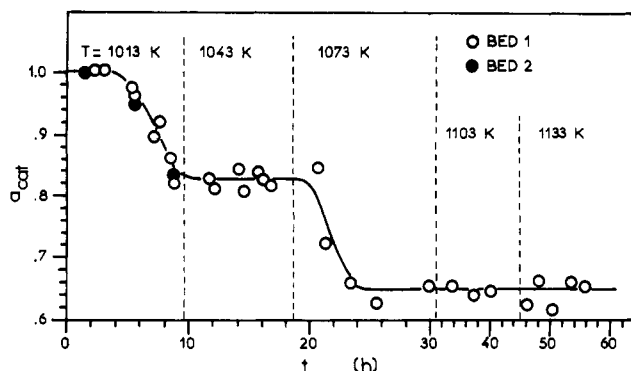


Figure 1. Dependence of the catalyst activity on the temperature and time of operation. Bed 1.

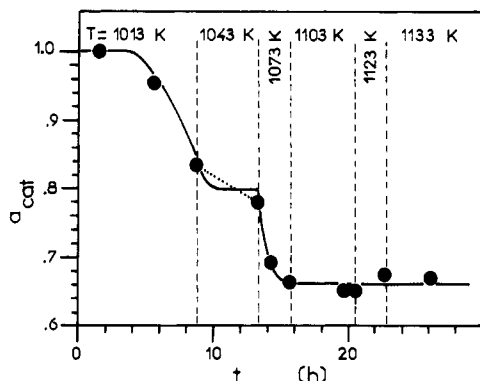


Figure 2. Dependence of the catalyst activity on the temperature and time of operation. Bed 2.

are observed: a first one, at 1013 K where  $\alpha_{\text{cat}} = 1$ , that lasted 3 h; a second one at 1043 K, where  $\alpha_{\text{cat}} = 0.80\text{--}0.82$ ; and a third one at 1073–1133 K, where  $\alpha_{\text{cat}} = (\alpha_{\text{cat}})_f = 0.65$ .

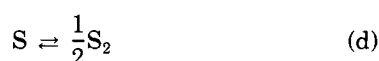
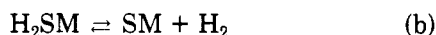
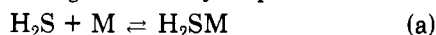
Differential thermal analysis in a nitrogen atmosphere did not show any difference between the fresh and the used catalyst. Chivers et al. (1980) state that no difference had been indicated by X-ray diffraction analysis between fresh and used catalyst particles.

The different activity levels revealed at 1013–1133 K can be attributed to irreversible phase transformations of  $\text{MoS}_2$  at high temperatures in hydrogen sulfide atmosphere.

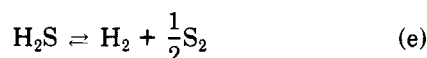
It is to be noted that after  $t_m$  the catalyst activity remained unchanged,  $\alpha_{\text{cat}} = (\alpha_{\text{cat}})_f = 0.65$ , for experimental runs at temperatures within the range of 1013–1133 K.

**Reaction Mechanism.** From the research on catalytic hydrosulfurization of petroleum fractions, it is generally accepted that the sulfur atoms of the organic molecules or hydrogen sulfide are adsorbed on the active sites (M) of the catalysts with n-type semiconductivity, like  $\text{MoS}_2$ .

A simple mechanism that can be attributed to the heterogeneous catalytic decomposition of hydrogen sulfide is given by the following elementary steps:



For these steps and for the whole reaction



the following conditions hold:

$$\begin{aligned} \Delta H_a < 0, \quad \Delta H_b > 0, \quad \Delta H_c > 0 \\ \Delta H_d = -52.1 \text{ kcal} \quad \text{and} \quad \Delta H_e = 21.7 \text{ kcal} \end{aligned} \quad (\text{f})$$

Table II. Rate Equations Derived from the Proposed Mechanism

model	rds	rate equation
1	a	$r_{w,\text{H}_2\text{S}} = \frac{k_{1,a} \left[ P_{\text{H}_2\text{S}} - \frac{1}{K_e} P_{\text{H}_2} P_{\text{S}_2}^{1/2} \right]}{1 + \frac{P_{\text{S}_2}^{1/2}}{K_c K_d} + \frac{P_{\text{H}_2} P_{\text{S}_2}^{1/2}}{K_b K_c K_d}} \quad (\text{A})$
2	b	$r_{w,\text{H}_2\text{S}} = \frac{k_{1,b} K_a \left[ P_{\text{H}_2\text{S}} - \frac{1}{K_e} P_{\text{H}_2} P_{\text{S}_2}^{1/2} \right]}{1 + K_a P_{\text{H}_2\text{S}} + \frac{P_{\text{S}_2}^{1/2}}{K_c K_d}} \quad (\text{B})$
3	c	$r_{w,\text{H}_2\text{S}} = \frac{k_{1,c} K_a K_b \left[ P_{\text{H}_2\text{S}} - \frac{1}{K_e} P_{\text{H}_2} P_{\text{S}_2}^{1/2} \right]}{P_{\text{H}_2} + K_a K_b P_{\text{H}_2\text{S}} + K_a P_{\text{H}_2} P_{\text{S}_2}^{1/2}} \quad (\text{C})$

at temperatures from 873 to 1223 K. The values of  $\Delta H_d$  and  $\Delta H_e$  have been computed from selected thermodynamic data (Kaloidas and Papayannakos, 1987).

This mechanism comprises the sorption of hydrogen sulfide molecules on the catalyst active sites (M), according to reaction a. The electron transfer from n-type semiconductor catalyst to sulfur atoms results in redistribution of the electrons of the system active site–hydrogen sulfide molecule, breakage of the bonds between sulfur and hydrogen atoms, development of bonds between hydrogen atoms, and finally desorption of hydrogen molecules as shown by reaction b. Sulfur is desorbed in monoatomic form (c) and reacts to diatomic molecules which constitute more than 97% mol/mol of the sulfur molecule system ( $\text{S}_1$ , ...,  $\text{S}_8$ ) (Kaloidas and Papayannakos, 1987).

A similar mechanism has been proposed by Zazhigalov et al. (1975) for the synthesis of  $\text{H}_2\text{S}$  in the presence of metal sulfides as catalysts.

**Rate Equations.** Considering as the rate-determining step (rds) one of the reactions a, b, or c of the proposed mechanism and using the Hougen–Watson formulation, three rate equations A, B, and C are derived, respectively, as given in Table II.

When one of the reactions a, b, or c is considered as the rds the other two plus (d) are considered at thermodynamic equilibrium. Equilibrium constants of reactions a, b, and c,  $K_a$ ,  $K_b$ , and  $K_c$ , have to be determined, while the values of the equilibrium constant of reaction d,  $K_d$ , are calculated from data given in the literature (Kaloidas and Papayannakos, 1987).

The influence of temperature on the kinetic parameters of the rate models are considered according to Arrhenius law. The equilibrium constants are described by the following thermodynamic equation:

$$K_j = \exp \left( -\frac{\Delta H_j}{RT} + \frac{\Delta S_j}{R} \right) \quad (\text{g})$$

where  $j = a, b, c, d$ , and e.

For the heats of reaction of the elementary steps the following equations are valid:

$$\begin{aligned} \Delta H_a + \Delta H_b + \Delta H_c + \Delta H_d &= \Delta H_e \\ \Delta H_j &= E_{1,j} - E_{2,j} \quad j = a, b, c, d \end{aligned} \quad (\text{h})$$

where  $E_{1,j}$  and  $E_{2,j}$  stand for activation energies of the forward and reverse reaction, respectively.

Consequently the rate equations can be written in the forms shown in Tables III–V. Thermodynamic restric-

**Table III. Rate Equation and Thermodynamic Restrictions of Model 1**

$$r_{w,H_2S} = \left[ k_{01,cat} \exp\left(-\frac{E_{1,cat}}{RT}\right) \left[ P_{H_2S} - \frac{1}{K_e} P_{H_2} P_{S_2}^{1/2} \right] \right] / \left[ 1 + KA_o \exp\left(-\frac{EA}{RT}\right) P_{S_2}^{1/2} + KB_o \exp\left(-\frac{EB}{RT}\right) P_{H_2} P_{S_2}^{1/2} \right] \quad (8)$$

$$k_{01,cat} = k_{01,a} \quad E_{1,cat} = E_{1,a}$$

$$KA_o = \exp\left(-\frac{\Delta S_c + \Delta S_d}{R}\right) \quad EA = -\Delta H_c - \Delta H_d$$

$$KB_o = \exp\left(-\frac{\Delta S_b + \Delta S_c + \Delta S_d}{R}\right) \quad EB = -\Delta H_b - \Delta H_c - \Delta H_d \quad (9)$$

restrictions:  $E_{1,cat} > 0$ ,  $EA < 52.1$  kcal/mol,  
 $EB < -21.7$  kcal/mol,  $EA > EB$

**Table IV. Rate Equation and Thermodynamic Restrictions of Model 2**

$$r_{w,H_2S} = \left[ k_{01,cat} \exp\left(-\frac{E_{1,cat}}{RT}\right) \left[ P_{H_2S} - \frac{1}{K_e} P_{H_2} P_{S_2}^{1/2} \right] \right] / \left[ 1 + KA_o \exp\left(-\frac{EA}{RT}\right) P_{H_2S} + KB_o \exp\left(-\frac{EB}{RT}\right) P_{S_2}^{1/2} \right] \quad (10)$$

$$k_{01,cat} = k_{01,b} \left( \frac{\Delta S_a}{R} \right) \quad E_{1,cat} = E_{1,b} + \Delta H_a$$

$$KA_o = \exp\left(\frac{\Delta S_a}{R}\right) \quad EA = \Delta H_a$$

$$KB_o = \exp\left(-\frac{\Delta S_c + \Delta S_d}{R}\right) \quad EB = -\Delta H_c - \Delta H_d \quad (11)$$

restrictions:  $E_{1,cat} > EB + 21.7$  kcal/mol,  $EA < 0$ ,  
 $EB < 52.1$  kcal/mol,  $EB > EA - 21.7$  kcal/mol

**Table V. Rate Equation, Parameters, and Thermodynamic Restrictions of Model 3**

$$r_{w,H_2S} = \left[ k_{01,cat} \exp\left(-\frac{E_{1,cat}}{RT}\right) \left[ P_{H_2S} - \frac{1}{K_e} P_{H_2} P_{S_2}^{1/2} \right] \right] / \left[ P_{H_2} + KA_o \exp\left(-\frac{EA}{RT}\right) P_{H_2S} + KB_o \exp\left(-\frac{EB}{RT}\right) P_{H_2} P_{H_2S} \right] \quad (12)$$

$$k_{01,cat} = k_{01,c} \exp\left(\frac{\Delta S_a + \Delta S_b}{R}\right) \quad E_{1,cat} = E_{1,c} + \Delta H_a + \Delta H_b$$

$$KA_o = \exp\left(\frac{\Delta S_a + \Delta S_b}{R}\right) \quad EA = \Delta H_a + \Delta H_b$$

$$KB_o = \exp\left(\frac{\Delta S_a}{R}\right) \quad EB = \Delta H_a \quad (13)$$

restrictions:  $E_{1,cat} > 73.8$  kcal/mol,  $EA < 73.8$  kcal/mol,  
 $EB < 0$ ,  $EA > EB$

tions for each model are derived from combination of (5), (9), (11), and (13). The restriction for positive values of activation energies  $E_{1,j}$  and  $E_{2,j}$  of the elementary steps is also applied.

**Mathematical Consideration of the Tubular Reactor.** The tubular reactor used in this study consisted of three parts: an empty part (E) in which only homogeneous decomposition occurred, a part (S) packed with  $\alpha$ -Al<sub>2</sub>O<sub>3</sub> particles (support of the catalyst bed) in the void volume

of which homogeneous decomposition occurred, and the catalyst bed. In the part of the catalyst bed, two parallel reactions occurred: one homogeneous in the particle voids and one catalytic on the catalyst surface.

For all parts of the reactor and the prevailing experimental conditions, the ideal plug flow pattern is applied as discussed in the Experimental Section.

The change of H<sub>2</sub>S conversion  $(\Delta x)_\lambda$  in an elementary reactor volume is calculated as

$$(\Delta x)_\lambda = (\Delta x_w)_\lambda + (\Delta x_\theta)_\lambda \quad (14)$$

For parts E and S the following equations are valid:

$$(\Delta x_w)_\lambda = 0 \quad (15)$$

$$(\Delta x_\theta)_\lambda = \epsilon_b \frac{A_d}{F_{0,H_2S}} (r_\theta)_\lambda (\Delta l)_\lambda \quad (16)$$

where  $\epsilon_b = 1$  for part E and  $\epsilon_b = 0.50$  for part S. The thermal, noncatalytic decomposition rates  $r_\theta$  of hydrogen sulfide in (16) are calculated by use of a previously developed kinetic model (Kaloidas and Papayannakos, 1989).

For an elementary volume of the catalyst bed (16) is valid using  $\epsilon_b = 0.45$ . The change of H<sub>2</sub>S catalytic conversion  $(\Delta x_w)_\lambda$  is calculated as

$$(\Delta x_w)_\lambda = \frac{A_d}{F_{0,H_2S}} d_b \alpha_{cat}(\eta)_\lambda (r_{w,H_2S})_\lambda (\Delta l)_\lambda \quad (17)$$

An iterative method (Kaloidas and Papayannakos, 1989) for the integration of the differential equations is used. The catalyst section length increment and the temperature gradual increment are under the restrictions

$$(\Delta l)_\lambda \leq 0.01 \text{ cm} \quad \text{and} \quad (\Delta T)_\lambda \leq 5 \text{ grad}$$

**Parameter Estimation and Model Discrimination.** The estimation of the parameters  $k_{01,cat}$ ,  $E_{1,cat}$ ,  $KA_o$ ,  $EA$ ,  $KB_o$ , and  $EB$  of the nonlinear models 1, 2, and 3 is carried out by minimization of either the objective functions

$$\begin{aligned} \text{of1} &= \sum_{i=1}^n (x_i - \hat{x}_i)^2 \\ \text{of2} &= \sum_{i=1}^n \left( 1 - \frac{\hat{x}_i}{x_i} \right)^2 \end{aligned} \quad (18)$$

according to Marquardt (1963) and the Levenberg algorithm (Himmelblau, 1970). The results are given in Tables VI and VII. Convergence was not accomplished in the case of model 2 when minimization of of2 was attempted.

The parameters estimated only for model 2 fulfill the restrictions presented in Tables III–V. However, the minimum values of of1 and of2 are comparable and the use of this criterion to select a model out of the three is not recommended. Thus, for design purposes, the use of any of the three models would be suitable.

The adequacy of the model 2 was tested by Fisher's criterion:

$$F_t = \frac{\hat{\sigma}_{res}^2}{\hat{\sigma}_e^2} = \frac{6.4 \times 10^{-6}}{3.5 \times 10^{-6}} = 1.8 < F_{0.95}^*(233,16) = 2.04$$

which ensures it.

From the estimated parameters of the proposed model 2, the following thermodynamic values of the elementary steps of the mechanism are calculated:

$$E_{1,b} = 51.9 \text{ kcal/mol}$$

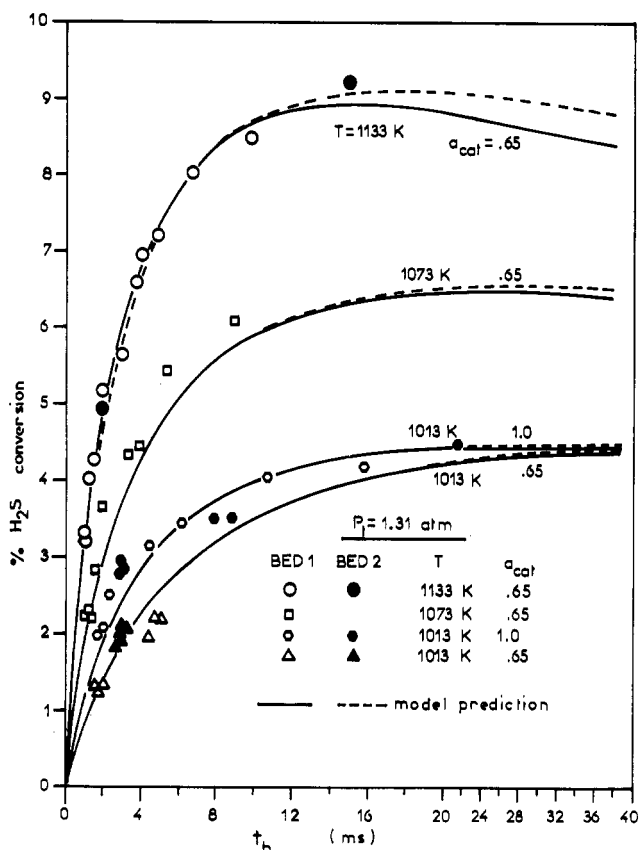
$$\Delta H_a = -51.5 \text{ kcal/mol}$$

$$\Delta H_b = 48.9 \text{ kcal/mol}$$

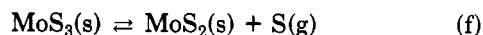
$$\Delta H_c = 76.4 \text{ kcal/mol}$$

**Table VI. Results of the Parameter Estimation of the Kinetic Models 1 and 3**

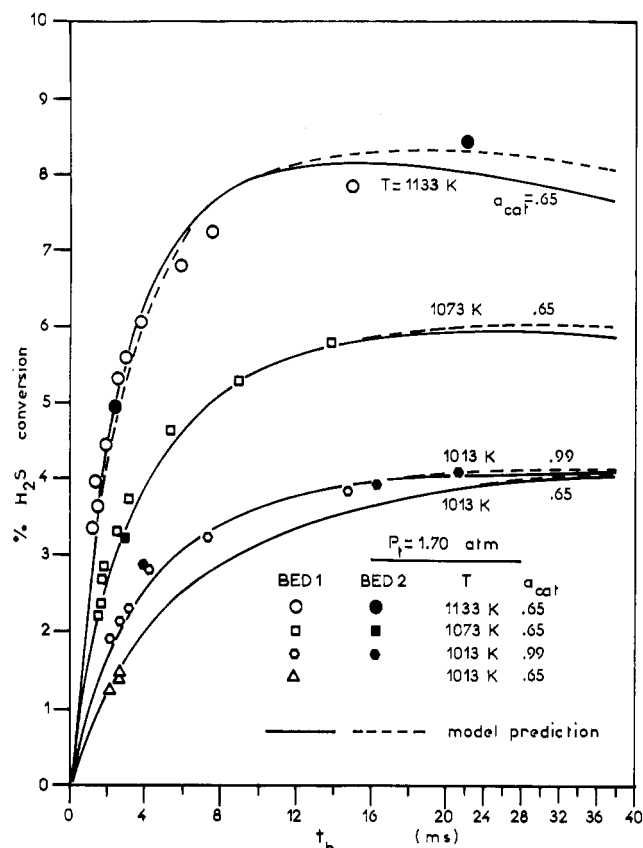
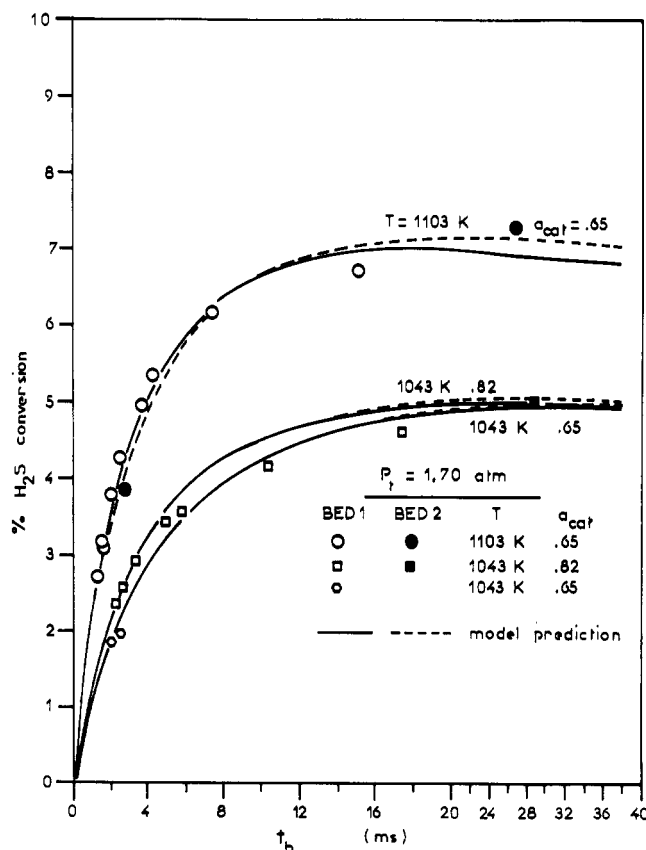
	of1	of2
<i>n</i>	239	239
<b>Model 1, Eq 8</b>		
$k_{01,cat}$ , mol/(g <sub>cat</sub> ·s·atm)	287.9	371.6
$E_{1,cat}$ , kcal/mol	29.48	30.10
$KA_0$ , atm <sup>-1/2</sup>	$4.018 \times 10^{36}$	$3.179 \times 10^{44}$
EA, kcal/mol	187.8	229.5
$KB_0$ , atm <sup>-3/2</sup>	$1.316 \times 10^{-2}$	$2.460 \times 10^{-2}$
EB, kcal/mol	-20.30	-19.12
$\sum_{i=1}^n (x_i - \hat{x}_i)^2$	$1.204 \times 10^{-3}$	$1.327 \times 10^{-3}$
$\sum_{i=1}^n \left(1 - \frac{\hat{x}_i}{x_i}\right)^2$	1.630	1.487
<b>Model 3, Eq 12</b>		
$k_{01,cat}$ , mol/(g <sub>cat</sub> ·s)	23.66	326.8
$E_{1,cat}$ , kcal/mol	31.60	37.06
$KA_0$	$3.547 \times 10^{-4}$	$7.681 \times 10^{-2}$
EA, kcal/mol	-7.918	3.091
$KB_0$ , atm <sup>-1</sup>	$1.008 \times 10^{54}$	$2.222 \times 10^{57}$
EB, kcal/mol	287.1	303.0
$\sum_{i=1}^n (x_i - \hat{x}_i)^2$	$1.346 \times 10^{-3}$	$1.398 \times 10^{-3}$
$\sum_{i=1}^n \left(1 - \frac{\hat{x}_i}{x_i}\right)^2$	1.562	1.493

**Figure 3.** H<sub>2</sub>S conversion vs catalyst bed space time.  $P_t = 1.31$  atm;  $T = 1013, 1073, 1133$  K.

The elementary step c of the proposed mechanism corresponds to the reaction



Thermodynamic data (Barin and Knacke, 1973) allow the calculation of enthalpy of formation of this reaction as  $\Delta H_f(298 \text{ K}) = 67.8 \text{ kcal/mol}$  and  $\Delta H_f(700 \text{ K}) = 69.0$

**Figure 4.** H<sub>2</sub>S conversion vs catalyst bed space time.  $P_t = 1.70$  atm;  $T = 1013, 1073, 1133$  K.**Figure 5.** H<sub>2</sub>S conversion vs catalyst bed space time.  $P_t = 1.70$  atm;  $T = 1043, 1103$  K.

kcal/mol. These values are very close to  $\Delta H_c$  estimated by model 2.

Figures 3-8 show the experimental data and the pre-

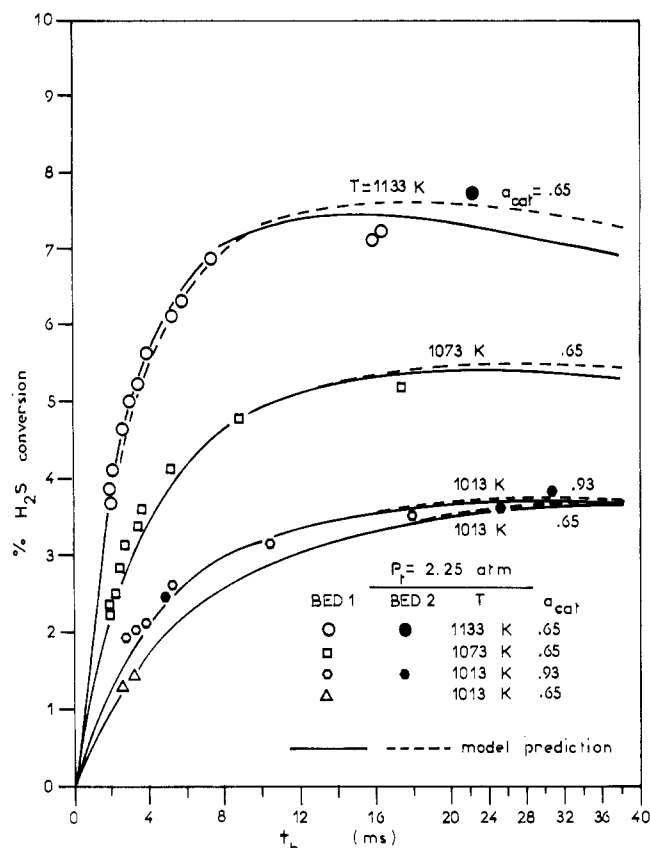


Figure 6.  $\text{H}_2\text{S}$  conversion vs catalyst bed space time.  $P_t = 2.25$  atm;  $T = 1013, 1073, 1133$  K.

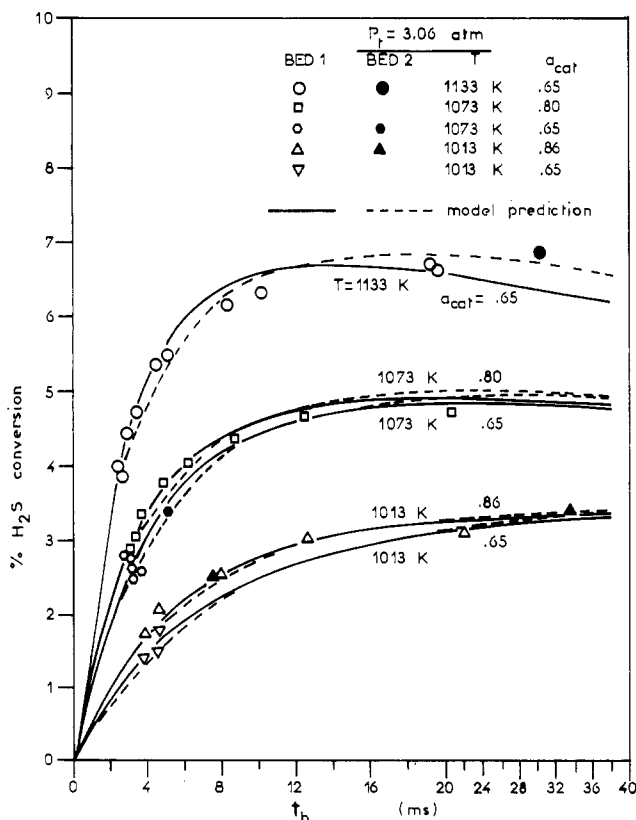


Figure 7.  $\text{H}_2\text{S}$  conversion vs catalyst bed space time.  $P_t = 3.06$  atm;  $T = 1013, 1073, 1133$  K.

dicted values for the proposed model 2. The comparisons are satisfactory for both catalyst beds. It is also indicated that diffusional limitations are negligible as discussed in the Experimental Section.

Table VII. Results of the Parameter Estimation of the Kinetic Model 2

	of 1
$n$	239 ( $n_+ = 112$ )
$n_p$	6
Model 2, Eq 10	
$k_{01, \text{cat}}, \text{mol}/(\text{g}_{\text{cat}} \cdot \text{s} \cdot \text{atm})$	43.37
$E_{1, \text{cat}}, \text{kcal/mol}$	0.4177
$K A_o, \text{atm}^{-1}$	$9.75 \times 10^{-7}$
$E A, \text{kcal/mol}$	-51.50
$K B_o, \text{atm}^{-1/2}$	17.03
$E B, \text{kcal/mol}$	-24.34
$\sum_{i=1}^n (x_i - \hat{x}_i)^2$	$1.488 \times 10^{-3}$
$\sum_{i=1}^n \left(1 - \frac{\hat{x}_i}{x_i}\right)$	1.528
$\sigma_{\text{res}} = \left[ \frac{\sum_{i=1}^n (x_i - \hat{x}_i)^2}{n - n_p} \right]^{1/2}$	$2.53 \times 10^{-3}$
$\left[ \frac{\sum_{i=1}^n \left(1 - \frac{\hat{x}_i}{x_i}\right)^2}{n - n_p} \right]^{1/2}$	0.0810
$(\sum_{i=1}^n x_i) / n$	0.0391
$\left[ \frac{\sum_{i=1}^n \left(x_i - \frac{\sum_{i=1}^n x_i}{n}\right)^2}{n - 1} \right]^{1/2}$	0.0170
$(\sum_{i=1}^n \hat{x}_i) / n$	0.0393
$\left[ \frac{\sum_{i=1}^n \left(x_i - \frac{\sum_{i=1}^n \hat{x}_i}{n}\right)^2}{n - 1} \right]^{1/2}$	0.0172

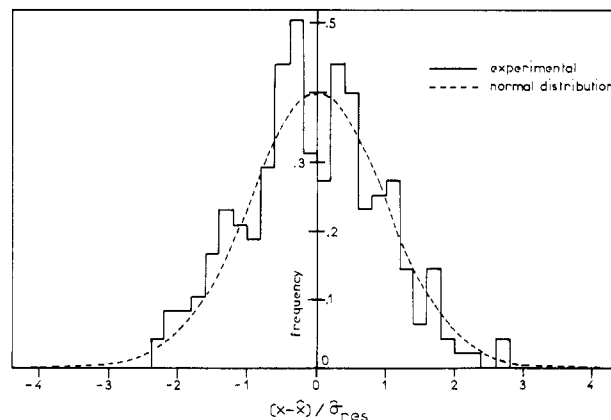


Figure 8. Histogram of the deviations of the experimental from the calculated  $\text{H}_2\text{S}$  conversions through model 2.

## Conclusions

The intrinsic kinetics of the catalytic decomposition of  $\text{H}_2\text{S}$ , over  $\text{MoS}_2$  as a catalyst, taking into account the reverse reaction of the  $\text{H}_2\text{S}$  synthesis was studied. The rate equation in Table IV corresponds to the proposed mechanism of  $\text{H}_2\text{S}$  dissociation and predicts well the  $\text{H}_2\text{S}$  con-

versions up to thermodynamic equilibrium at the conditions of experimentation. The proposed mechanism indicates that the rate-controlling step is the elementary step b which describes the breakage of hydrogen-sulfur bonds of the hydrogen sulfide molecules adsorbed on the catalyst active sites. The activation energy of this step was calculated as 51.9 kcal/mol. The catalytic activity of MoS<sub>2</sub> for the H<sub>2</sub>S decomposition is time and temperature dependent. It is irreversibly stabilized at temperatures greater than 1073 K and the remaining activity is 0.65.

## Nomenclature

$A_d$  = tubular reactor cross section area, cm<sup>2</sup>  
 $b_{cat}$  = auxiliary undimensional quantity as defined by (4)  
 $C_{in}$ ,  $C_{out}$  = reactant concentrations at fixed bed inlet and output, respectively, mol/L  
 $D_{e,H_2S}$  = effective diffusion coefficient of H<sub>2</sub>S in the catalytic particle pores, cm<sup>2</sup>/s  
 $d_p$  = particle diameter, cm  
 $d_b$  = catalyst bed apparent density, g/cm<sup>3</sup>  
 $d_r$  = reactor internal diameter, cm  
 $E_{1j}$ ,  $E_{2j}$  = activation energies of forward and reverse reactions  $j$  ( $j = a, b, c, d$ ), respectively, kcal/mol  
 $E_{1,cat}$  = apparent activation energy of the catalytic H<sub>2</sub>S decomposition reaction, kcal/mol  
 $EA$ ,  $EB$  = inhibition parameters of the models as they are defined by (9), (11), and (13), kcal/mol  
 $F_{0,H_2S}$  = H<sub>2</sub>S molar feed flow rate, mol/s  
 $F_t$  =  $F$  distribution variable  
 $F^*_{0.95}(df1, df2)$  = value of the  $F$  distribution variable corresponding to probability 0.95 (significance level 0.05) with numerator and denominator degrees of freedom  $df1$  and  $df2$ , respectively  
 $K_j$  = thermodynamic equilibrium constants of the reactions  $j$  ( $j = a, b, c, d, e$ ), respectively  
 $KA_o$ ,  $KB_o$  = inhibition parameters of the rate equations defined by (9), (11), and (13) (units dependent on the model)  
 $k_{1,j}$  = specific rate of the forward reaction  $j$  ( $j = a, b, c$ ) (units dependent on the reaction)  
 $k_{01,j}$  = frequency factors corresponding to the specific rates  $k_{1,j}$   
 $k_{01,cat}$  = apparent frequency factor of the forward catalytic H<sub>2</sub>S decomposition, mol/(g<sub>cat</sub>·s·atm)  
 $L_{cat}$  = catalyst bed length, cm  
 $M$  = active site of the catalyst  
 $n$  = number of experimental runs  
 $n_o$  = reaction order  
 $n_p$  = number of the estimated parameters  
 $n_+$  = number of positive deviations ( $x - \hat{x}$ )  
 $of1$ ,  $of2$  = objective functions as defined by (18)  
 $P_t$  = total pressure of the reactant system, atm  
 $P_A$  = partial pressure of a reactant species A ( $A = H_2S, H_2, S_2$ ), atm  
 $Pe_L$ ,  $Pe_r$  = axial and radial fixed bed Peclet numbers, respectively  
 $R$  = gas constant, kcal/(mol·K)  
 $Re_p$  = Reynolds number based on particle diameter  
 $r_\theta$  = thermal, noncatalytic, H<sub>2</sub>S decomposition rate, mol/(s·cm<sup>3</sup>)  
 $r_{w,H_2S}$  = catalytic H<sub>2</sub>S decomposition rate based on catalyst mass, mol/(s·g<sub>cat</sub>)  
 $rds$  = rate-determining step  
 $T$  = catalyst bed temperature, K  
 $t$  = time of catalyst operation, h  
 $t_b$  = catalyst bed space time, ms  
 $t_m$  = operation time after which the catalyst activity remains constant, h  
 $V_{cat}$  = catalyst bed volume, cm<sup>3</sup>  
 $x$ ,  $\hat{x}$  = experimentally determined and model predicted H<sub>2</sub>S conversion values, respectively

## Greek Letters

$\alpha_{cat}$  = remaining activity of catalyst  
 $(\alpha_{cat})_f$  = final constant catalyst activity  
 $\Delta H_j$  = enthalpy of the reaction  $j$  ( $j = a, b, c, d, e$ ), kcal  
 $(\Delta l)_\lambda$  = elementary reactor length, cm  
 $\Delta S_j$  = entropy change of the reaction  $j$  ( $j = a, b, c, d, e$ ), kcal/K  
 $(\Delta T)_\lambda$  = temperature difference in  $(\Delta l)_\lambda$ , K  
 $(\Delta x)_\lambda$  = change of H<sub>2</sub>S conversion in  $(\Delta l)_\lambda$   
 $(\Delta x_\theta)_\lambda$  = change of H<sub>2</sub>S thermal, noncatalytic conversion in  $(\Delta l)_\lambda$   
 $(\Delta x_w)_\lambda$  = change of H<sub>2</sub>S catalytic conversion in  $(\Delta l)_\lambda$   
 $\delta_{cat}$  = catalyst particle tortuosity  
 $\epsilon_b$  = fixed bed void fraction  
 $(\eta)_\lambda$  = effectiveness factor of catalyst particles in  $(\Delta l)_\lambda$   
 $\sigma_{res}^2$  = variance of the residuals  
 $\sigma_e^2$  = variance of the reproducibility of the experiments

## Subscripts

$i$  = with respect to the  $i$ th experimental run  
 $j$  = with respect to the  $j$ th reaction  
 $\lambda$  = with respect to the  $\lambda$ th elementary division of the reactor length

**Registry No.** H<sub>2</sub>S, 7783-06-4; MoS<sub>2</sub>, 1317-33-5.

## Literature Cited

- Barin, I.; Knacke, O. *Thermochemical Properties of Inorganic Substances*; Springer: Berlin, 1973; pp 491, 648.  
 Carberry, J. J. *Chemical and Catalytic Reaction Engineering*; McGraw-Hill: New York, 1976; pp 143-193.  
 Chivers, T.; Hyne, J. B.; Lau, C. The Thermal Decomposition of Hydrogen Sulfide over Transition Metal Sulfides. *Int. J. Hydrogen Energy* 1980, 5(5), 499-506.  
 Froment, G. F.; Bischoff, K. B. *Chemical Reactor Analysis and Design*; Wiley: New York, 1979; pp 592-661.  
 Fukuda, K.; Dokiya, M.; Kameyama, T.; Kotera, Y. Catalytic Decomposition of Hydrogen Sulfide. *Ind. Eng. Chem. Fundam.* 1978, 17(4), 243-248.  
 Himmelfrau, D. M. *Process Analysis by Statistical Methods*; Wiley: New York, 1979; Chapter 6.  
 Kaloidas, V. Technical Kinetic Studies on the Thermal and Catalytic Decomposition of Hydrogen Sulphide to Hydrogen and Sulphur. Ph.D. Thesis, National Technical University of Athens, Greece, 1988.  
 Kaloidas, V. E.; Papayannakos, N. G. Hydrogen Production from the Decomposition of Hydrogen Sulphide. Equilibrium Studies on the System H<sub>2</sub>S/H<sub>2</sub>/S<sub>i</sub> ( $i=1, \dots, 8$ ) in the Gas Phase. *Int. J. Hydrogen Energy* 1987, 12(6), 403-409.  
 Kaloidas, V.; Papayannakos, N. Kinetics of Thermal, Non-Catalytic Decomposition of Hydrogen Sulphide. *Chem. Eng. Sci.* 1989, 44(11), 2493-2500.  
 Kingman, F. E. T. Decomposition of Hydrogen Sulfide and Water on Molybdenum Filaments. *Trans. Faraday Soc.* 1936, 32, 903-907.  
 Kotera, Y.; Todo, N.; Fukuda, K. Method for Manufacture of Hydrogen and Carbonyl Sulfide from Hydrogen Sulfide and Carbon Monoxide. U.S. Patent 3 856 925, 1974.  
 Kotera, Y.; Todo, N.; Fukuda, K. Process for Production of Hydrogen and Sulfur from Hydrogen Sulfide as Raw Material. U.S. Patent 4 039 613, 1977.  
 Marquardt, D. W. An Algorithm for Least-Squares Estimation of Non-Linear Parameters. *J. Soc. Ind. Appl. Math.* 1963, 11(2), 431-441.  
 Pascal, P. *Nouveau Traite de Chimie Mineral*; Masson et Cie: Paris, 1960; Tome XIII, pp 939-1028.  
 Rase, H. F. *Chemical Reactor Design for Process Plants. Vol. 1. Principles and Techniques*; Wiley: New York, 1977; pp 222-234.  
 Raymont, M. E. D. The Thermal Decomposition of Hydrogen Sulphide. Ph.D. Thesis, The University of Calgary, Alberta, Canada, 1974.  
 Raymont, M. E. D. Make Hydrogen from Hydrogen Sulfide. *Hydrocarbon Process.* 1975, 54(7), 139-142.  
 Zashigalov, V. A.; Gerei, S. V.; Rubanik, M. Ya. Relationships in the Catalytic Reaction between Hydrogen and Sulfur in the presence of Metal Sulfides. I. *Kinet. Katal.* 1975, 16(4), 967-974.

Received for review March 22, 1990

Revised manuscript received August 15, 1990

Accepted August 28, 1990